catalysts

MDPI

Article

Catalytic Abatement of Nitrous Oxide Coupled with Ethane Oxydehydrogenation over Mesoporous Cr/Al_2O_3 Catalyst

Yan Zhang, Suresh Kumar Megarajan, Xia Xu, Jingting Lu and Heqing Jiang *

Qingdao Key Laboratory of Functional Membrane Material and Membrane Technology, Qingdao Institute of Bioenergy and Bioprocess Technology, Chinese Academy of Sciences, Qingdao 266101, China; zhangyan@qibebt.ac.cn (Y.Z.); suresh@qibebt.ac.cn (S.K.M.); xuxia@qibebt.ac.cn (X.X.); lujt@qibebt.ac.cn (J.L.)
* Correspondence: jianghq@qibebt.ac.cn; Tel./Fax: +86-532-80662716

Academic Editors: Shaobin Wang and Xiaoguang Duan
Received: 21 March 2017; Accepted: 25 April 2017; Published: 4 May 2017

Abstract: Waste nitrous oxide (N_2O) was utilized as an oxidant for ethane oxydehydrogenation reaction at the temperature range from 450 °C to 700 °C over the mesoporous Cr/Al_2O_3 catalyst synthesized via the one-pot evaporation-induced self-assembly (EISA) method. The catalyst was characterized by X-ray diffraction, transmission electron microscopy, and nitrogen adsorption-desorption analysis. The obtained mesoporous material with favorable textural property and advantageous thermal stability was investigated as the catalyst for ethane oxydehydrogenation. It was found that the utilization of N_2O as an oxidant for the oxydehydrogenation reaction of ethane resulted in simultaneous and complete N_2O abatement. Moreover, the catalytic conversion of C_2H_6 to C_2H_4 was increased from 18% to 43% as the temperature increased from 450 °C to 700 °C. The increased N_2O concentration from 5 vol % to 20 vol % resulted in an increased ethane conversion but decreased ethylene selectivity because the nonselective reactions occurred. Ethane was converted into ethylene with approximately 51% selectivity and 22% yield at 700 °C and N_2O concentration of 10%. After a catalytic steady state was reached, no obvious decline was observed during a 15 h evaluation period.

Keywords: evaporation-induced self-assembly; ordered mesopores; Cr/Al_2O_3 oxide; N_2O decomposition; ethane oxydehydrogenation

1. Introduction

Nitrous oxide (N_2O), a waste by-product and an environmental pollutant generated mainly from anthropogenic emissions and industrial processes such as adipic acid and nitric acid plants, has more than 300 times greater potential than CO_2 to cause global warming and ozone depletion [1]. The abatement of N_2O has thus been a topic of environmental relevance. The concentration of N_2O for environmental catalytic after-treatment usually varies from 0 vol % to 50 vol %, and the N_2O abatement in adipic acid production has been most effectively tackled due to the high concentration and limited point source [2]. Among various commercial N_2O removal technologies, the catalytic or thermal decomposition of N_2O was widely applied. Based on the conversion of N_2O to N_2 and O_2 reaction, the oxygen species characterized with different reactivity and different thermal stability [3,4] were formed, making N_2O an excellent optional oxidant for many oxidation reactions. Solutia Inc. employed N_2O as an oxidant, and this technology has recently been commercialized to produce phenol from benzene [5,6]. Kondratenko et al. [7] and Novoveska et al. [8] also used N_2O as an oxidant for the production of propene from oxidative dehydrogenation of propane, and it seems to be one of the promising and most elegant methods for the transformation of light paraffins to olefins. In this regard,

a process that combines the N_2O abatement with the simultaneous production of valuable chemical fuels would be environmentally and economically attractive, and also reveals a new perspective for the utilization of light paraffins.

Catalytic dehydrogenation of light alkanes is of important significance since it upgrades low cost paraffins feedstock into valuable olefins product [9–11]. Nowadays, ethane dehydrogenation has become a crucial way to meet the increasing demand of ethylene, which can be used to synthesize polymers, ethane oxide, and many other basic and intermediate products [12]. Supported chromium oxide catalysts were found to be effective for alkane dehydrogenation, among which a Cr/Al_2O_3 catalyst has been used for years on a commercial scale [9–11]. Former experimental and theoretical studies reported that the carbon deposit was identified as the main source for the deactivation of supported chromia catalysts during alkane dehydrogenation reaction [13,14]. Sullivan et al. [15] investigated the process of coke deposition over chromia-alumina during propane dehydrogenation using in-situ UV Raman spectroscopy analysis. They observed the polynuclear aromatic hydrocarbons and polyenes when reaction temperature was relatively low (400 °C), and the conjugated olefins when increasing the temperature to >500 °C. Nowadays, there is an increasing body of evidence that the introduction of mesoporosity into the catalyst material could be a way to solve the deactivation of the catalyst due to carbonaceous deposits [16–19]. Hartmann et al. [17], Schwieger et al. [18], and Su et al. [19] introduced a substantial amount of mesopores into the microporous structured zeolite of Fe/ZSM-5, and an improved catalyst longevity was obtained during the oxidation of benzene to phenol process.

In this contribution, a highly active and stable chromia-alumina catalyst was proposed, and the textural properties were determined. A well-developed mesoporous structure and a relatively high surface area of the present material were presented. In addition, nitrous oxide was utilized as an oxidant for the ethane oxydehydrogenation reaction in the presence of mesoporous chromia-alumina catalyst. Our concept is based on the combination of the exothermic N_2O decomposition with the thermal dehydrogenation of ethane, with the aim to completely remove the N_2O and simultaneously the production of C_2H_4 from C_2H_6.

2. Results

The small angle X-ray diffraction is a useful tool for studying the ordered mesoporous material and has been widely used to access the structure of a sample [20,21]. Figure 1 displays the small angle XRD pattern of the as-prepared Cr/Al_2O_3. A strong [1 0 0] diffraction peak around 1.1° was presented, indicating the formation of p6mm two-dimensional hexagonal ordered mesoporous structure. The wide-angle XRD pattern of Cr/Al_2O_3 is shown in the inset of Figure 1. Two broad peaks were obtained at the ranges of 10°–40° and 50°–80°, respectively, illustrating the formation of the mesoporous γ-Al_2O_3 phase. It should be pointed out that no apparent XRD signal of a chromium-based compound was detected, indicating the high dispersion of chromium species among the mesoporous skeleton of the γ-Al_2O_3 material. The obtained long-range ordered mesoporous structure was further confirmed by the TEM results, as expressly displayed in Figure 2. The alignment of cylindrical pores were distinctly observed along [1 1 0] direction (Figure 2a,b), and the hexagonal arrangement of pores were typical highly ordered along [0 0 1] direction (Figure 2b). It is noteworthy that no additional isolated chromium-based particle was detected over the entire network, and the introduction of Cr via the one-pot EISA method did not destroy the mesoporous structure of alumina, which is consistent with the XRD characterization results. The combination of the XRD and TEM results convinced us that the ordered mesoporous Cr/Al_2O_3 was easily obtained and the mesoporous framework was successfully preserved after 700 °C calcination, demonstrating good thermal stability.

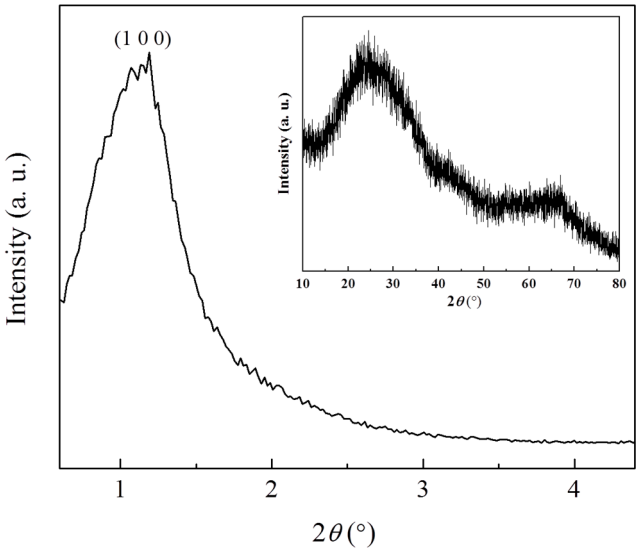

Figure 1. Small-angle and wide-angle (inset) X-ray diffraction patterns of Cr/Al_2O_3.

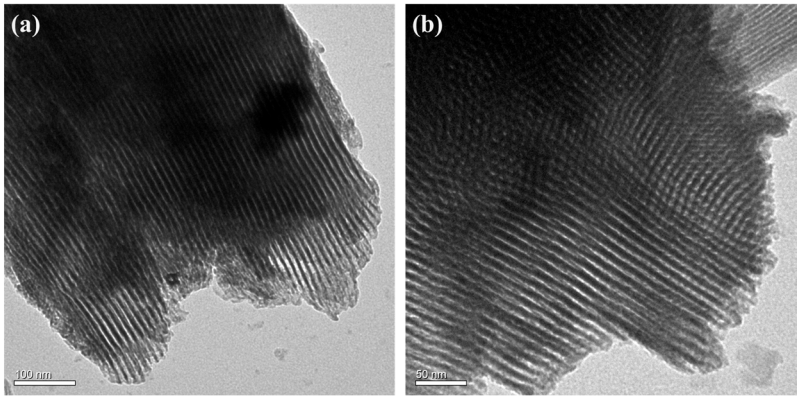

Figure 2. Transmission electron microscopy (TEM) images of as-synthesized Cr/Al_2O_3 material. (**a**) TEM image viewed along [1 1 0] orientation. (**b**) TEM image viewed along [1 1 0] and [0 0 1] orientations.

The formation of mesoporous Cr/Al_2O_3 was also supported by nitrogen adsorption-desorption analysis. Figure 3 shows the nitrogen adsorption and desorption isotherms as well as the pore size distribution as an inset. As shown in Figure 3, the sample calcined at 700 °C gave type IV curve with H1-shaped hysteresis loop, which was the typical feature of ordered mesoporous materials with uniform mesopores [22,23] among the framework of the Cr/Al_2O_3 material. The deduction of H1-shaped hysteresis loops in Figure 3 further confirmed the cylindrical pores along [1 1 0] in TEM analysis. Furthermore, after being calcined at 700 °C, Cr/Al_2O_3 had a large BET surface area of 205 $m^2\ g^{-1}$ and a pore volume of 0.34 $cm^3\ g^{-1}$. In addition, the pore size distribution exhibited in the inset of Figure 3 was extremely narrow, and the position of the peak was located in 5.2 nm. The large surface area and narrow pore size distribution of this ordered mesoporous alumina-based material, in combination with the advantageous thermal stability, enhance its potential applications in catalysis.

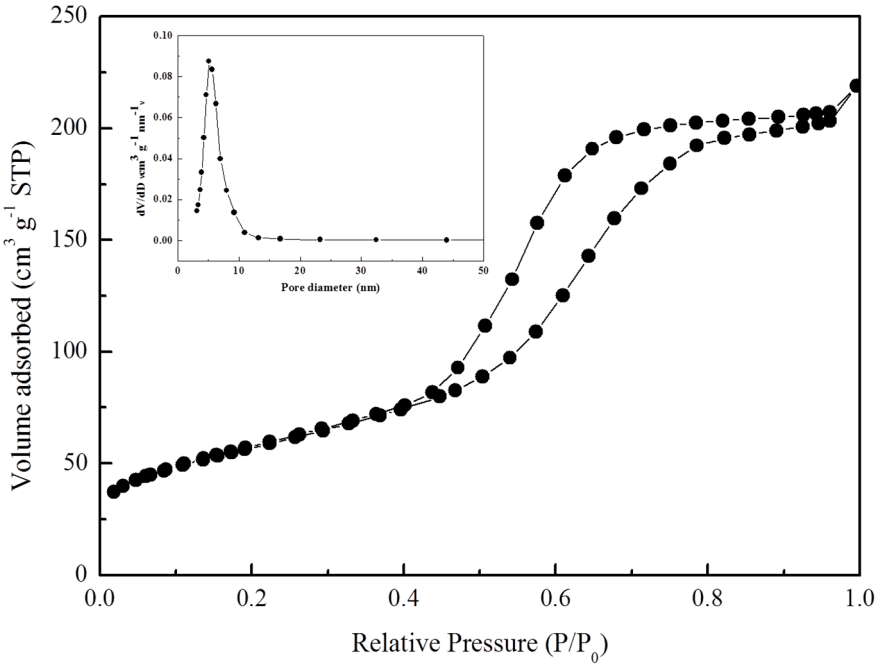

Figure 3. N_2 adsorption isotherms and pore size distribution curve (inset) of Cr/Al_2O_3.

The XPS spectrum for fresh Cr/Al_2O_3 catalyst in the Cr 2p binding energy region is shown in Figure 4. The experimental curve was fitted with two characteristic peaks centered at 577.1 and 579.5 eV, typical of the corresponding Cr^{3+} and Cr^{6+} species [24,25], respectively. This indicated the presence of chromium with two oxidation states, and the calculated Cr^{6+}/Cr^{3+} ratio was 2.23, demonstrating that most chromium species existed as Cr^{6+} in the fresh Cr/Al_2O_3 catalyst.

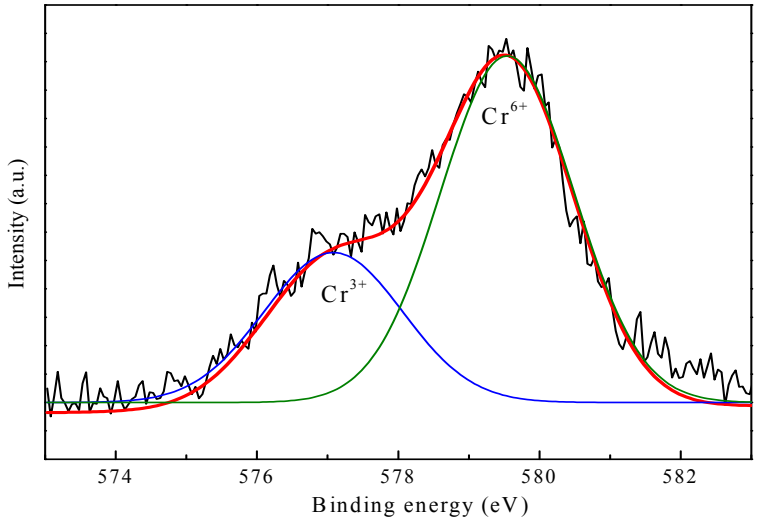

Figure 4. X-ray photoelectron spectra (XPS) spectrum for the fresh Cr/Al_2O_3 catalyst.

The catalytic performance of the mesoporous Cr/Al_2O_3 material in N_2O abatement with simultaneous C_2H_4 production from the oxydehydrogenation of C_2H_6 at various temperatures is shown in Figure 5. It is seen that the N_2O conversion (X_{N2O}) to N_2 was completed (100%) in the whole temperature range, simultaneously the catalytic conversion of C_2H_6 (X_{C2H6}) to C_2H_4 was increased from 18% to 43% with the increasing temperature from 450 °C to 700 °C. This catalytic activity was higher than that of the bulk Cr_2O_3 (<3% ethane conversion at 650 °C) and the mesoporous

silica-supported chromium oxide catalyst (8.2%–18.7% ethane conversion) for ethane dehydrogenation reported by Sayari et al. [14]. For ethane oxydehydrogenation using N_2O as an oxidant, Held et al. [26] investigated the catalytic properties over iron modified different zeolite (ZSM-5, H-Y, mordenite) catalysts. The comparison results indicated that the catalytic performance of mesoporous Cr/Al_2O_3 herein was lower than that of Fe/ZSM-5, whereas it was superior to the iron modified faujasite and mordenite catalysts.

In the reaction medium, N_2O was expected to be partly utilized for ethane oxydehydrogenation or for direct decomposition to N_2 and O_2. In the present work, no O_2 signal was recorded, indicating that all the oxygen species were involved in the reactions. According to the investigations from Pérez-Ramirez et al. [27] and Wang et al. [28], the decomposition of N_2O over the active site led to the formation of reactive oxygen species, the removal of which from the surface of catalyst is a rate determining step. When C_2H_6 is used as a reductant, the generated oxygen species participate in oxidation of C_2H_6, one could herein conclude that the Cr/Al_2O_3 catalyst should be responsible not only for N_2O decomposition but also for the ethane oxydehydrogenation. Moreover, a distinctly higher N_2O conversion than ethane oxydehydrogenation occurred, which can be ascribed to the nonselective heterogeneous reactions of a portion of oxygen with C_2H_6/C_2H_4 to form CO_x during ethane oxydehydrogenation reaction. This is also consistent with the observations by Held et al. [26]. Furthermore, the ethylene selectivity was reaction temperature depended. As shown in Figure 5, only 4%–17% of C_2H_4 selectivity (S_{C2H4}) was observed at 450–550 °C, while higher C_2H_4 selectivity was obtained with increasing operating temperature to 600–700 °C. For example, ethylene selectivity of 51% with 22% ethylene yield (Y_{C2H4}) was achieved at 700 °C. Considering the complete N_2O conversion in the whole temperature range, the ratio of generated oxygen to reaction intermediates (activated C_2H_6) over the catalyst surface was temperature-dependent. At lower temperatures (450–550 °C), the significantly higher ratio of generated oxygen to reaction intermediates led to nonselective oxidation of C_2H_6/C_2H_4 to CO_x, and low ethylene selectivity was obtained. At higher temperatures (600–700 °C), more ethane was activated over the catalyst surface that decreased the ratio of generated oxygen to intermediates, and further increased the ethylene selectivity. In addition, more oxygen species that can selectively convert ethane to ethylene were probably produced at higher temperatures. However, future work should be conducted to gain further understanding of this system.

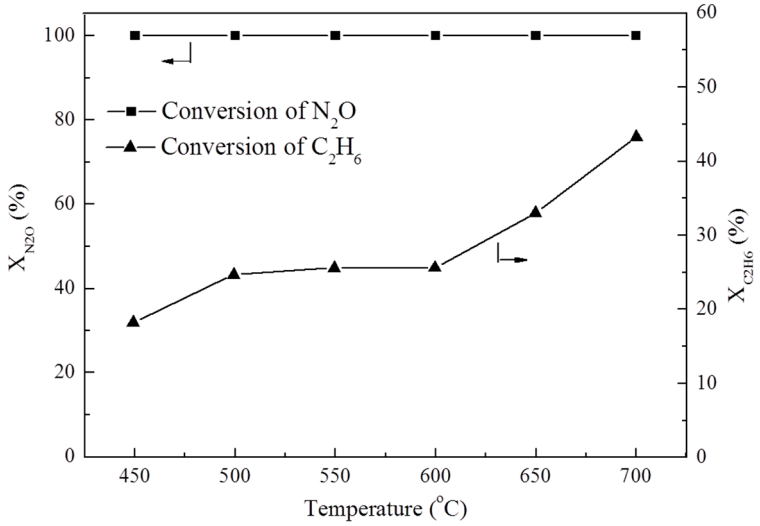

Figure 5. *Cont.*

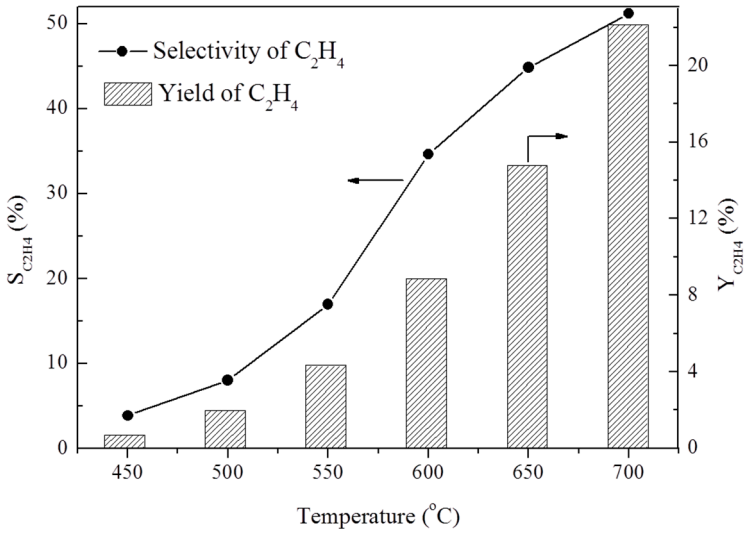

Figure 5. Catalytic performance of Cr/Al_2O_3 for ethane oxydehydrogenation using N_2O as an oxidant. Reaction conditions: T = 450–700 °C, Flow rate = 25 mL min^{-1}, C_2H_6 concentration = 10 vol %, N_2O concentration = 10 vol %, He as a balance.

The structure properties of the spent material after catalytic characterization (Figure 5) were characterized in Figure 6 to estimate the thermal stability of mesoporous chromia-alumina catalyst. The XRD pattern (Figure 6a) showed two broad peaks typical of γ-Al_2O_3 phase, and no obvious chromium-based peak was observed, which is similar to the corresponding fresh sample in Figure 1. Moreover, as depicted in Figure 6b, the highly ordered mesoporous framework was found to be comparable with the fresh catalyst displayed in Figure 2. These findings indicated that the spent catalyst retained its structure properties even after the reaction from 450 °C to 700 °C, further confirming the good thermal stability of mesoporous Cr/Al_2O_3 catalyst.

The XPS spectrum for the spent catalyst shown in Figure 7 revealed two peaks centered at 577.2 and 579.6 eV due to the presence of both Cr^{3+} and Cr^{6+} species [24,25]. However, a decreased Cr^{6+}/Cr^{3+} ratio of 0.12 was calculated. These results suggested that a Cr^{6+}/Cr^{3+} redox cycle was actively involved in the ethane oxydehydrogenation using N_2O as an oxidant, and most of the active Cr^{6+} species (Figure 4) converted to the lower oxidant state Cr^{3+} during the reaction.

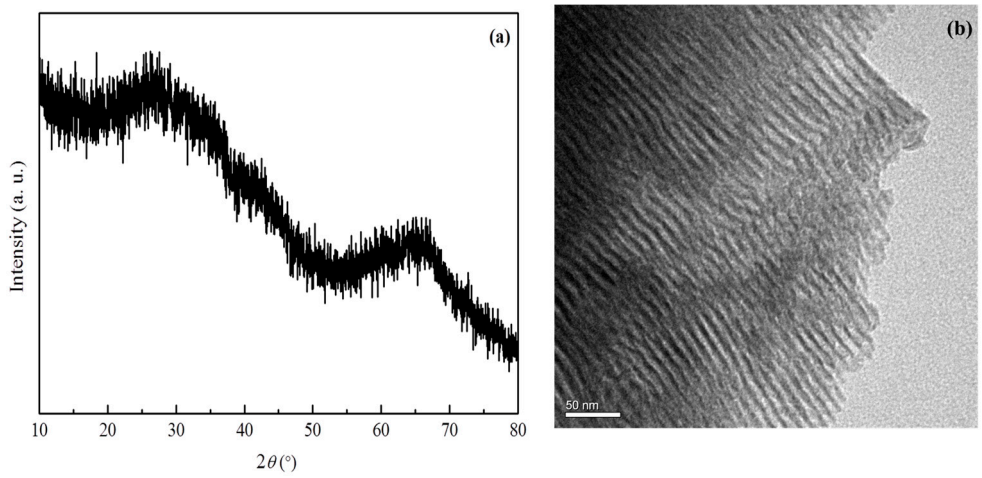

Figure 6. Wide-angle X-ray diffraction pattern (**a**) and TEM image (**b**) for the spent Cr/Al_2O_3 catalyst.

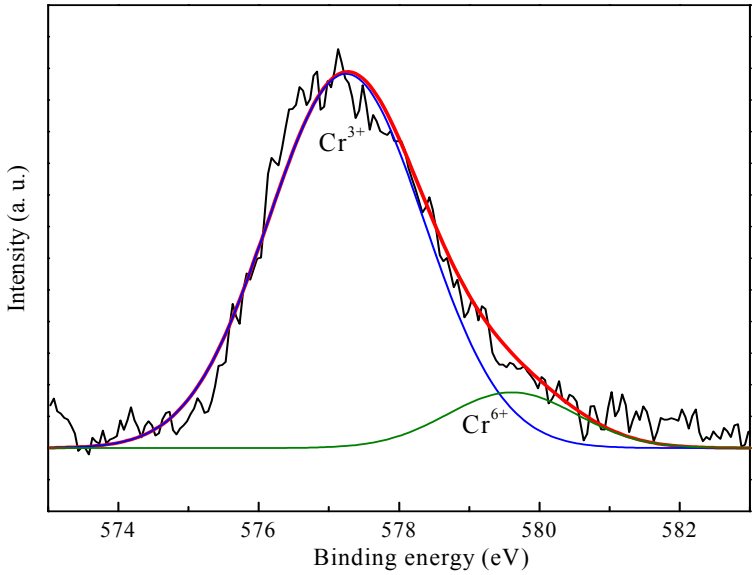

Figure 7. XPS spectrum for the spent Cr/Al_2O_3 catalyst.

The ethane dehydrogenation reaction was investigated over the Cr/Al_2O_3 catalyst at 700 °C in the absence of N_2O, and a dramatic activity decay was observed upon extending the operation time (not shown), which can be attributed to the coke deposition during the reaction. In order to suppress the coke formation, N_2O was employed as an oxidant for ethane oxydehydrogenation in the present study. The influence of N_2O concentration on the ethane oxydehydrogenation reaction at 700 °C is displayed in Figure 8. It was found that the C_2H_6 conversion increased from 31% to 54% when changing the N_2O concentration from 5 vol % to 20 vol %, which can be ascribed to the formation of more oxygen species from N_2O decomposition in the case of a higher N_2O concentration. In contrast, a decreased selectivity of ethylene was observed since the higher ratio of oxygen species favored the nonselective reactions (C_2H_6/C_2H_4 oxidation to CO_x). Therefore, a higher ethane conversion was always compromised with a lower ethylene selectivity. In this regard, the fluctuation of ethylene yield (17.8%–20.1%) was not distinct at different N_2O concentrations, as shown in Figure 8.

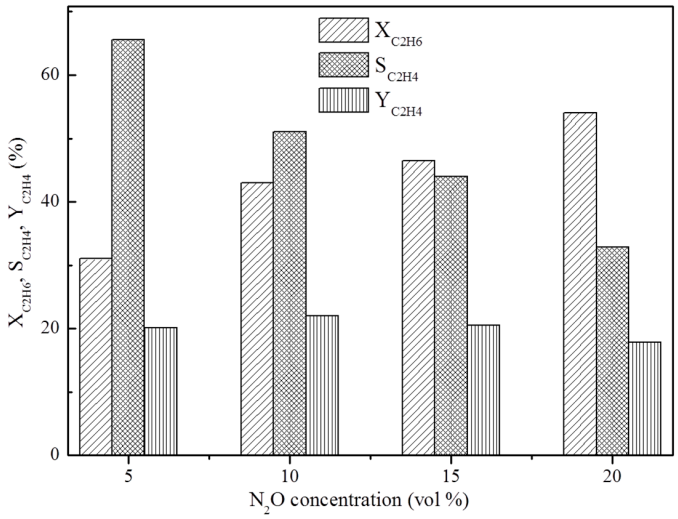

Figure 8. Effect of N_2O concentration on ethane oxydehydrogenation over the mesoporous Cr/Al_2O_3 catalyst. Reaction conditions: T = 700 °C, Flow rate = 25 mL min^{-1}, C_2H_6 concentration = 10 vol %, N_2O concentration = 5–20 vol %, He as a balance.

Figure 9 exemplifies the profiles of the C_2H_6 conversion, and the selectivity and yield of C_2H_4 product as a function of time-on-stream over mesoporous Cr/Al_2O_3 catalyst. Before analysis, the catalyst was run under the feed gas with 10 vol % C_2H_6 and 5 vol % N_2O at a flow rate of 25 mL min^{-1} at 700 °C for about 6 h to reach a steady state of the catalytic performance. Compared to the initial data after 40 min of feed gas treatment (Figure 8), it was found that the catalytic activity drops to a certain degree during 6 h testing, after which no noticeable deactivation of the catalyst was observed during a 15 h evaluation period. It gives an ethane conversion of approximately 30%, a selectivity for ethylene of 58%, and an ethylene yield of 17%, demonstrating the good stability of the mesoporous Cr/Al_2O_3 catalyst, which is a key parameter regarding to the catalyst development. In view of the above results, the process of using N_2O as an oxidant for ethane oxydehydrogenation in the presence of mesoporous Cr/Al_2O_3 catalyst may be considered not only as a useful way to functionalize light paraffin but also as an effective procedure for N_2O abatement.

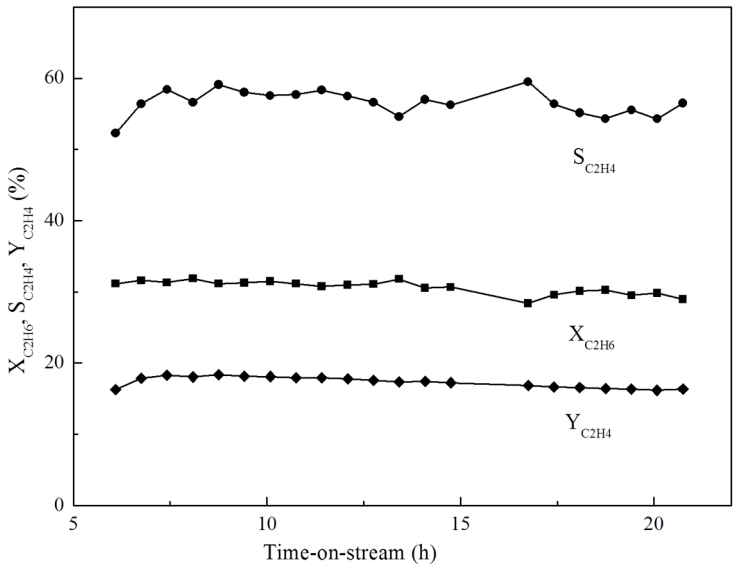

Figure 9. Time-on-stream profiles of the C_2H_6 conversion, the C_2H_4 selectivity, and the C_2H_4 yield. Reaction conditions: T = 700 °C, Flow rate = 25 mL min^{-1}, C_2H_6 concentration = 10 vol %, N_2O concentration = 5 vol %, He as a balance.

3. Experimental

3.1. Catalyst Preparation

The mesoporous Cr/Al_2O_3 with 5% molar fraction of chromium was prepared via the evaporation-induced self-assembly (EISA) route as reported [29–31]. Here, the $(EO)_{20}(PO)_{70}(EO)_{20}$ triblock copolymer (Pluronic P123) was used as a structure directing agent. Typically, Pluronic P123 (5.0 g, Sigma-Aldrich Co. LLC., St. Louis, MO, USA) was dissolved in 100 mL of anhydrous ethanol at room temperature. After small vortex stirring for 4 h, 8.0 mL of 67 wt % HNO_3 (Sinopharm Chemical Reagent Co. Ltd., Shanghai, China) and 2.5 mmol of chromium nitrate nonahydrate ($Cr(NO_3)_3{\cdot}9H_2O$, Sinopharm Chemical Reagent Co. Ltd., Shanghai, China, ≥99%), and 47.5 mmol aluminum isopropoxide (Sigma-Aldrich Co. LLC., St. Louis, MO, USA, 98%) were added into the above solution. The total amount of metal species (50 mmol for 5.0 g of P123) was kept constant. After vigorous stirring at room temperature for about 12 h, solvent evaporation was carried out at 60 °C for about 48 h in a drying oven. The resultant solid was homogenized by grinding, and calcined under air atmosphere for 4 h at 400 °C in a muffle furnace (heating rate 1 °C min^{-1}). The above sample was further treated at 700 °C for 4 h (3 °C min^{-1} ramping rate), and the final Cr_2O_3-Al_2O_3 catalyst obtained was denoted as Cr/Al_2O_3 in present description.

3.2. Catalyst Characterization

Powder X-ray diffraction (XRD) images of the sample were collected at room temperature by a Bruker D8 ADVANCE diffractometer using a Cu Kα radiation source. The small angle XRD pattern was collected at the ranges from 0.6° to 4.4°, and the wide angle one was from 10° to 80°. Transmission electron microscopy (TEM) photos were recorded on a Hitachi H-7650 transmission electron microscope with an EDS detector with a 100 kV working voltage. Nitrogen adsorption-desorption isotherms were obtained with an Autosorb iQ instrument at −196 °C. Prior to the characterization, the sample was degassed under vacuum (1×10^{-5} Torr) at 200 °C for about 6 h. The surface area was calculated using the Brunauer-Emmett-Teller (BET) method. The Barrett-Joyner-Halenda (BJH) method was utilized to calculate the pore size distribution with Kruk-Jaroniec-Sayari (KJS) correction [22]. The pore volume was calculated based on the volume of liquid nitrogen adsorbed at approximately $p/p_0 = 1$. The X-ray photoelectron spectra (XPS) were collected on an ESCALAB MKII spectrometer with a Mg Kα radiation ($h\nu$ = 1253.6 eV).

3.3. Activity Test

The catalytic activity on ethane oxidative dehydrogenation using N_2O as an oxidant was estimated in a fixed-bed corundum reactor under atmospheric pressure. A quantity of 250 mg of a catalyst was used as the prepared powder and was fixed in the middle section of the reactor. Before the reaction, the catalyst was pretreated at 450 °C with flowing helium for 30 min. A reacting feed gas at a flow rate of 25 mL min^{-1} containing 10 vol % of C_2H_6, 5–20 vol % of N_2O, and balance He was passed through the catalyst bed. The mass flow controllers (Bronkhorst, The Netherlands) were used to control all the gas flows. The composition of outlet gas was analyzed online with an Agilent 7890B gas chromatograph equipped with a thermal conductivity detector (TCD). Before the analysis of outlet gas, the reaction proceeded for 40 min at each temperature or each gas concentration. The total gas flow rate at outlet (F_{out}) was calculated by using N as an internal standard. N_2O conversion, ethane conversion, and selectivity and yield of the product were calculated by the following equations:

$$X(N_2O) = \frac{F^{in}_{total} \times C^{in}_{N_2O} - F^{out}_{total} \times C^{out}_{N_2O}}{F^{in}_{total} \times C^{in}_{N_2O}} \times 100\% \quad (1)$$

$$X(C_2H_6) = \frac{F^{in}_{total} \times C^{in}_{C_2H_6} - F^{out}_{total} \times C^{out}_{C_2H_6}}{F^{in}_{total} \times C^{in}_{C_2H_6}} \times 100\% \quad (2)$$

$$S(C_2H_4) = \frac{F^{out}_{total} \times C^{out}_{C_2H_4}}{F^{in}_{total} \times C^{in}_{C_2H_6} - F^{out}_{total} \times C^{out}_{C_2H_6}} \times 100\% \quad (3)$$

$$Y(C_2H_4) = \frac{X(C_2H_6) \times S(C_2H_4)}{100}\% \quad (4)$$

4. Conclusions

(1) Ordered mesoporous Cr/Al_2O_3 composite oxide was facilely synthesized via an evaporation-induced self-assembly strategy. Characterization results revealed that the obtained material possessed excellent textual properties and thermal stabilities.

(2) Ordered mesoporous Cr/Al_2O_3 was utilized as the catalyst for ethane oxydehydrogenation using N_2O as an oxidant. This mesoporous catalyst displayed a prominent activity for N_2O abatement with 100% conversion over the whole temperature range. Moreover, an improved catalytic property for C_2H_6 oxydehydrogenation was exhibited with the increased reaction temperatures. A maximal per pass C_2H_6 conversion of 43% and C_2H_4 yield of 22% were obtained at 700 °C.

(3) When feeding N_2O from the concentration of 5 vol % to 20 vol %, a higher ratio of generated oxygen was provided, and an accordingly significant enhancement of C_2H_6 conversion and declination of C_2H_4 selectivity can be detected.

(4) The mesoporous Cr/Al_2O_3 catalyst was successfully operated at 700 °C for 15 h with fairly stable performance.

Acknowledgments: Financial support from the National Natural Science Foundation of China (21606249, 21550110496), the Shandong Provincial Natural Science Foundation, China (BS2014NJ003), Project funded by China Postdoctoral Science Foundation (2015M582158) is greatly acknowledged.

Author Contributions: Yan Zhang and Heqing Jiang conceived and designed the experiments; Suresh Kumar Megarajan and Jingting Lu and Xia Xu performed the experiments; Yan Zhang and Suresh Kumar Megarajan analyzed the data; Yan Zhang wrote the draft and Heqing Jiang improved it.

Conflicts of Interest: The authors declare no conflict of interest.

References

1. Kondratenko, E.V.; Ovsitser, O. Catalytic abatement of nitrous oxide coupled with selective production of hydrogen and ethylene. *Angew. Chem. Int. Ed.* **2008**, *47*, 3227–3229. [CrossRef] [PubMed]
2. Kapteijn, F.; Rodriguez-Mirasol, J.; Moulijn, J.A. Heterogeneous catalytic decomposition of nitrous oxide. *Appl. Catal. B* **1996**, *9*, 25–64. [CrossRef]
3. Panov, G.I.; Uriarte, A.K.; Rodkin, M.A.; Sobolev, V.I. Generation of active oxygen species on solid surfaces. Opportunity for novel oxidation technologies over zeolites. *Catal. Today* **1998**, *41*, 365–385. [CrossRef]
4. Ates, A.; Reitzmann, A. Transient multi pulse method for the determination of N_2O-interaction with ZSM-5 type zeolites. *React. Kinet. Catal. Lett.* **2005**, *86*, 11–20. [CrossRef]
5. Panov, G.I. Advances in oxidation catalysis; Oxidation of benzene to phenol by nitrous oxide. *CATTECH* **2000**, *4*, 18–31. [CrossRef]
6. Uriarte, A.K. Nitrous oxide (N_2O)-Waste to value. *Stud. Surf. Sci. Catal.* **2000**, *130*, 743–748.
7. Pérez-Ramírez, J.; Kondratenko, E.V. Steam-activated FeMFI zeolites as highly efficient catalysts for propane and N_2O valorisation via oxidative conversions. *Chem. Commun.* **2003**, *9*, 2152–2153. [CrossRef]
8. Bulanek, R.; Wichterlova, B.; Novoveska, K.; Kreibich, V. Oxidation of propane with oxygen and/or nitrous oxide over Fe-ZSM-5 with low iron concentrations. *Appl. Catal. A* **2004**, *264*, 13–22. [CrossRef]
9. Weckhuysen, B.M.; Schoonheydt, R.A. Alkane dehydrogenation over supported chromium oxide catalysts. *Catal. Today* **1999**, *51*, 223–232. [CrossRef]
10. Bhasin, M.M.; McCain, J.H.; Vora, B.V.; Imai, T.; Pujado, P.R. Dehydrogenation and oxydehydrogenation of paraffins to olefins. *Appl. Catal. A* **2001**, *221*, 397–419. [CrossRef]
11. Sanfilippo, D.; Miracca, I. Dehydrogenation of paraffins: Synergies between catalyst design and reactor engineering. *Catal. Today* **2006**, *111*, 133–139. [CrossRef]
12. Gärtner, C.A.; van Veen, A.C.; Lercher, J.A. Oxidative dehydrogenation of ethane: common principles and mechanistic aspects. *ChemCatChem* **2013**, *5*, 3196–3217. [CrossRef]
13. Rao, T.V.M.; Yang, Y.; Sayari, A. Ethane dehydrogenation over pore-expanded mesoporous silica supported chromium oxide: 1. Catalysts preparation and characterization. *J. Mol. Catal. A* **2009**, *301*, 152–158. [CrossRef]
14. Rao, T.V.M.; Zahidi, E.M.; Sayari, A. Ethane dehydrogenation over pore-expanded mesoporous silica supported chromium oxide: 2. Catalytic properties and nature of active sites. *J. Mol. Catal. A* **2009**, *301*, 159–165. [CrossRef]
15. Sullivan, V.S.; Stair, P.C.; Jackson, S.D. Catalysis in applications. In *Proceedings of International Symposium on Applied Catalysts*, 1st ed.; Jackson, S.D., Hargreaves, J.S.J., Lennon, D., Eds.; The Royal Society of Chemistry: London, UK, 2003; pp. 32–41.
16. Wu, L.L.; Degirmenci, V.; Magusin, P.C.M.M.; Lousberg, N.J.H.G.M.; Hensen, E.J.M. Mesoporous SSZ-13 zeolite prepared by a dual-template method with improved performance in the methanol-to-olefins reaction. *J. Catal.* **2013**, *298*, 27–40. [CrossRef]
17. Hartmann, M. Hierarchical zeolites: A proven stategy to combine shape selectivity with efficient mass transport. *Angew. Chem. Int. Ed.* **2004**, *43*, 5880–5882. [CrossRef] [PubMed]
18. Lopez-Orozco, S.A.; Inayat, A.; Schwab, A.; Selvam, T.; Schwieger, W. Zeolitic Materials with Hierarchical Porous Structures. *Adv. Mater.* **2011**, *23*, 2602–2615. [CrossRef] [PubMed]

19. Chen, L.H.; Li, X.Y.; Rooke, J.C.; Zhang, Y.H.; Yang, X.Y.; Tang, Y.; Xiao, F.S.; Xiao, B.L. Hierarchically structured zeolites: synthesis, mass transport properties and applications. *J. Mater. Chem.* **2012**, *22*, 17381–17403. [CrossRef]
20. Beck, J.S.; Vartuli, J.C.; Roth, W.J. A new family of mesoporous molecular sieves prepared with liquid crystal templates. *J. Am. Chem. Soc.* **1992**, *114*, 10834–10843. [CrossRef]
21. Kresge, C.T.; Leonowicz, M.E.; Roth, W.J. Ordered mesoporous molecular sieves synthesized by a liquid-crystal template mechanism. *Nature* **1992**, *359*, 710–712. [CrossRef]
22. Kruk, M.; Jaroniec, M.; Sayari, A. Application of large pore MCM-41 molecular sieves to improve pore size analysis using nitrogen adsorption measurements. *Langmuir* **1997**, *13*, 6267–6273. [CrossRef]
23. Xu, L.L.; Song, H.L.; Chou, L.J. One-pot synthesis of ordered mesoporous NiO-CaO-Al_2O_3 composite oxides for catalyzing CO_2 reforming of CH_4. *ACS Catal.* **2012**, *2*, 1331–1342. [CrossRef]
24. Khatib, S.J.; Fierro, J.L.G.; Bañares, M.A. Effect of phosphorous additive on the surface chromium oxide species on alumina for propane oxidation to propylene. *Top. Catal.* **2009**, *52*, 1459–1469. [CrossRef]
25. Shee, D.; Sayari, A. Light alkane dehydrogenation over mesoporous Cr_2O_3/Al_2O_3 catalysts. *Appl. Catal. A* **2010**, *389*, 155–164. [CrossRef]
26. Held, A.; Kowalska, J.; Nowińska, K. Nitrous oxide as an oxidant for ethane oxydehydrogenation. *Appl. Catal. B* **2006**, *64*, 201–208. [CrossRef]
27. Kondratenko, E.V.; Pérez-Ramírez, J. Oxidative functionalization of propane over FeMFI zeolites: Effect of reaction variables and catalyst constitution on the mechanism and performance. *Appl. Catal. A* **2004**, *267*, 181–189. [CrossRef]
28. Liu, H.F.; Wei, Y.Y.; Caro, J.; Wang, H.H. Oxidative coupling of methane with high C_2 yield by using chlorinated perovskite $Ba_{0.5}Sr_{0.5}Fe_{0.2}Co_{0.8}O_{3-\delta}$ as catalyst and N_2O as oxidant. *ChemCatChem* **2010**, *2*, 1539–1542. [CrossRef]
29. Yuan, Q.; Yin, A.X.; Luo, C.; Sun, L.D.; Zhang, Y.W.; Duan, W.T.; Liu, H.C.; Yan, C.H. Facile synthesis for ordered mesoporous γ-aluminas with high thermal stability. *J. Am. Chem. Soc.* **2008**, *130*, 3465–3472. [CrossRef] [PubMed]
30. Morris, S.M.; Fulvio, P.F.; Jaroniec, M. Ordered mesoporous alumina-supported metal oxides. *J. Am. Chem. Soc.* **2008**, *130*, 15210–15216. [CrossRef] [PubMed]
31. Lu, J.T.; Zhang, Y.; Jiao, C.L.; Megarajan, S.K.; Gu, D.; Yang, G.C.; Jiang, H.Q.; Jia, C.J.; Schüth, F. Effect of reduction-oxidation treatment on structure and catalytic properties of ordered mesoporous Cu-Mg-Al composite oxides. *Sci. Bull.* **2015**, *60*, 1108–1113. [CrossRef]